Cyclooxygenase-2 is instrumental in Parkinson's disease neurodegeneration

Peter Teismann*, Kim Tieu*, Dong-Kug Choi*, Du-Chu Wu*, Ali Naini*, Stéphane Hunot†, Miquel Vila*, Vernice Jackson-Lewis*, and Serge Przedborski*‡§¶

*Neuroscience Research Laboratories of the Movement Disorder Division, Department of Neurology, ‡Department of Pathology, and §Center for Neurobiology and Behavior, Columbia University, New York, NY 10032; and †Institut National de la Santé et de la Recherche Médicale U289, Hôpital de la Salpêtière, 75013 Paris, France

Edited by Richard D. Palmiter, University of Washington School of Medicine, Seattle, WA, and approved February 14, 2003 (received for review December 11, 2002)

Parkinson's disease (PD) is a neurodegenerative disorder of uncertain pathogenesis characterized by the loss of the nigrostriatal dopaminergic neurons, which can be modeled by the neurotoxin 1-methyl-4-phenyl-1,2,3,6-tetrahydropyridine (MPTP). Increased expression of cyclooxygenase type 2 (COX-2) and production of prostaglandin E_2 have been implicated in neurodegeneration in several pathological settings. Here we show that COX-2, the rate-limiting enzyme in prostaglandin E_2 synthesis, is up-regulated in brain dopaminergic neurons of both PD and MPTP mice. COX-2 induction occurs through a JNK/c-Jun-dependent mechanism after MPTP administration. We demonstrate that targeting COX-2 does not protect against MPTP-induced dopaminergic neurodegeneration by mitigating inflammation. Instead, we provide evidence that COX-2 inhibition prevents the formation of the oxidant species dopamine-quinone, which has been implicated in the pathogenesis of PD. This study supports a critical role for COX-2 in both the pathogenesis and selectivity of the PD neurodegenerative process. Because of the safety record of the COX-2 inhibitors, and their ability to penetrate the blood–brain barrier, these drugs may be therapies for PD.

Parkinson's disease (PD) is a common neurodegenerative disease characterized by disabling motor abnormalities, which include tremor, muscle stiffness, paucity of voluntary movements, and postural instability (1). Its main neuropathological feature is the loss of the nigrostriatal dopamine-containing neurons, whose cell bodies are in the substantia nigra pars compacta (SNpc) and nerve terminals in the striatum (2). Except for a handful of inherited cases related to known gene defects, PD is a sporadic condition of unknown pathogenesis (1).

Epidemiological studies suggest that inflammation increases the risk of developing a neurodegenerative condition such as Alzheimer's disease (3). In keeping with this suggestion, inflammatory processes associated with increased expression of the enzyme cyclooxygenase type 2 (COX-2) and elevated levels of prostaglandin E_2 (PGE_2) have been implicated in the cascade of deleterious events leading to neurodegeneration in a variety of pathological settings (4–6). COX converts arachidonic acid to PGH_2, the precursor of PGE_2 and several other prostanoids, and exists in eukaryotic cells in two main isoforms: COX-1, which is constitutively expressed in many cell types; and COX-2, which is normally not present in most cells, but whose expression can readily be induced in inflamed tissues (7). Although both isoforms synthesize PGH_2, COX-1 is primarily involved in the production of prostanoids relevant to physiological processes, whereas COX-2 is mainly responsible for the production of prostanoids linked to pathological events (7).

In this study, we asked whether PD is associated with COX-2 up-regulation, and, if so, whether COX-2 expression contributes to the PD neurodegenerative process. We found that COX-2 expression is induced specifically within SNpc dopaminergic neurons in postmortem PD specimens and in the 1-methyl-4-phenyl-1,2,3,6-tertrahydropyridine (MPTP) mouse model of PD during the destruction of the nigrostriatal pathway. We also show that COX-2 induction occurs through a JNK/c-Jun-dependent mechanism and that COX-2 ablation and inhibition attenuate MPTP-induced nigrostriatal dopaminergic neurodegeneration, not by curtailing inflammation, but possibly by mitigating oxidative damage. These findings provide compelling evidence that COX-2 is involved in the pathogenesis of PD and suggest a potential mechanism for the selectivity of neuronal loss in this disease.

Materials and Methods

Animals and Treatments. Wild-type mice were 8-week-old C57/BL/6 specimens (Charles River Breeding Laboratories). *Ptgs1*$^{-/-}$ mice deficient in COX-1 (B6;129P2-Ptgs1^{tm1}), *Ptgs2*$^{-/-}$ mice deficient in COX-2 (B6;129P2-Ptgs2^{tm1}), and their respective wild-type littermates were obtained from Taconic Farms. Genotyping was performed by PCR (8). For each study, 4–10 mice per group received four i.p. injections of MPTP·HCl (20 mg/kg free base; Sigma) dissolved in saline, 2 h apart in one day, and were killed at selected times ranging from 0 to 7 days after the last injection. Control mice received saline only. MPTP handling and safety measures were in accordance with our published guidelines (9). Rofecoxib (12.5–50 mg per kg per day; a gift from Merck Frosst Labs, Pointe Claire, PQ, Canada) was given to mice by gavage for 5 days before and after MPTP-injection. Control mice received vehicle only. This regimen was well tolerated and yielded 0.40 ± 0.06 ng of rofecoxib per mg of tissue (mean ± SEM for five mice) 2 h after the last gavage (measurements were kindly performed by Pauline Luk from Merck Frosst by HPLC with UV detection). Rofecoxib inhibited MPTP-induced PGE_2 production in a dose-dependent manner and did not affect striatal 1-methyl-4-phenylpyridinium (MPP^+) levels in mice (see Tables 2 and 3, which are published as supporting information on the PNAS web site, www.pnas.org). JNK pathway inhibitor CEP-11004 (1 mg/kg; gift from Cephalon, West Chester, PA) was given to mice by s.c. injections 1 day before and 6 days after MPTP-injection as described (10); CEP-11004 did not affect striatal MPP^+ levels in mice (see Table 3). Control mice received the vehicle only. This protocol was in accordance with National Institutes of Health guidelines for the use of live animals and was approved by the Institutional Animal Care and Use Committee of Columbia University.

RNA Extraction and RT-PCR. Total RNA was extracted from selected mouse brain regions as described (11). The primer sequences for COX-1, COX-2, IL-1β-converting enzyme (ICE), the 91-kDa subunit of NADPH oxidase (gp91), macrophage antigen complex-1 (MAC-1), inducible nitric oxide synthase (iNOS), and GAPDH can be found in refs. 4 and 11. All products were quantified by a phosphorimager (Bio-Rad) or a FluorChem 8800 digital image system (Alpha Innotech, San Leandro, CA).

This paper was submitted directly (Track II) to the PNAS office.

Abbreviations: PD, Parkinson's disease; MPTP, 1-methyl-4-phenyl-1,2,3,6-tetrahydropyridine; PG, prostaglandin; COX, cyclooxygenase; SNpc, substantia nigra pars compacta; MPP^+, 1-methyl-4-phenylpyridinium; MAC-1, macrophage antigen complex-1; TH, tyrosine hydroxylase; ICE, IL-1β converting enzyme; iNOS, inducible NO synthase.

¶To whom correspondence should be addressed at: Departments of Neurology and Pathology, BB-307, Columbia University, 650 West 168th Street, New York, NY 10032. E-mail: sp30@columbia.edu.

Immunoblots. Mouse and human brain protein extracts were prepared as described (4); for phosphorylated c-Jun analysis, isolating mixture also contained 50 mM NaF and 1 mM Na_3VO_4. Western blot analyses were performed as described (4). Primary antibodies used were as follows: COX-2 (1:250; Transduction Laboratories, Lexington, KY), COX-1 (1:250; Santa Cruz Biotechnology), phosphorylated c-Jun (1:200; Cell Signaling, Beverly, MA), total c-Jun (1:200; Santa Cruz Biotechnology), or β-actin (1:10,000; Sigma). A horseradish-peroxidase-conjugated secondary antibody (1:500–1:25,000; Amersham Pharmacia) and a chemiluminescent substrate (SuperSignal Ultra; Pierce) were used for detection. Bands were quantified by using a FluorChem 8800 digital image system (Alpha Innotech).

PGE_2 Tissue Content. PGE_2 content was assessed in mouse and human tissues by a commercially available high sensitivity chemiluminescence enzyme immunoassay (EIA) kit (4) from Cayman Chemical, Ann Arbor, MI, according to the manufacturer's instructions.

COX-2, Tyrosine Hydroxylase (TH), Glial Fibrillary Acidic Protein (GFAP), and MAC-1 Immunohistochemistry. These were all performed according to our standard protocol for single or double immunostaining (11). Primary antibodies were COX-1 (1:100; Santa Cruz Biotechnology), COX-2 (1:250; gift from W. L. Smith, Michigan State University, East Lansing), TH (1:500; Chemicon), GFAP (1:500; Chemicon), and MAC-1 (1:1,000; Serotec). Immunostaining was visualized by 3,3′-diaminobenzidine with or without nickel enhancement or by fluorescein and Texas red (Vector Laboratories) and was examined by either regular light or confocal microscopy.

TH immunostaining was carried out on striatal and midbrain sections (11) and the TH- and Nissl-stained SNpc neurons were counted by stereology using the optical fractionator method described (11). The striatal density of TH immunoreactivity was determined as described (11).

Measurement of Protein-Bound 5-Cysteinyl-dopamine. Quantification of protein-bound 5-cysteinyl-dopamine was achieved by HPLC with electrochemical detection (12) using mouse brain extracts at 2 and 4 days after MPTP injections.

MPTP Metabolism. Striatal MPP^+ levels were determined by HPLC-UV detection (wavelength, 295 nm; ref. 11) 90 min after the fourth i.p. injection of 20 mg/kg MPTP. Synaptosomal uptake of $[^3H]MPP^+$ was performed as before (11) in *Ptgs2*$^{+/+}$ and *Ptgs2*$^{-/-}$ littermates.

Human Samples. Human samples were obtained from the Parkinson brain bank at Columbia University. Selected PD and controls samples were matched for age at death and interval from death to tissue processing (see *Supporting Text*, which is published as supporting information on the PNAS web site, for details).

Statistical Analysis. All values are expressed as the mean ± SEM. Differences among means were analyzed by using one- or two-way ANOVA with time, treatment, or genotype as the independent factor. When ANOVA showed significant differences, pairwise comparisons between means were tested by Newman–Keuls post hoc testing. In all analyses, the null hypothesis was rejected at the 0.05 level.

Results

MPTP Induces COX-2 Expression and Activity in Mouse Ventral Midbrain. To determine whether the expression of COX isoforms is affected during the nigrostriatal neurodegeneration, we assessed the contents of COX-1 and COX-2 mRNA and protein in ventral midbrains (the brain region that contains the SNpc) of saline- and MPTP-injected mice, at different time points. Ventral midbrain COX-1 mRNA and protein were detected in saline-treated mice and their contents were not significantly changed by MPTP administration (Fig. 1 *A*, *B*, *D*, and *E*); there was a decrease of COX-1 mRNA (but not of protein) at 2 and 4 days after MPTP administration, suggesting a transient reduction in COX-1 transcription because of the toxic insult. In contrast, ventral midbrain COX-2 mRNA and protein were almost undetectable in saline-treated mice (Fig. 1 *A*, *C*, *D*, and *F*), but were detected in MPTP-treated mice at 24 h after injections and thereafter (Fig. 1 *A*, *C*, *D*, and *F*). To determine whether MPTP-related COX-2 up-regulation paralleled an increase of its enzymatic activity, we quantified tissue contents of PGE_2. Ventral midbrain PGE_2 is detectable in saline-injected mice, and, as shown by the use of *Ptgs2*$^{-/-}$ and *Ptgs1*$^{-/-}$ mice, derives primarily from COX-1 (see Table 2). Ventral midbrain PGE_2 contents rose during MPTP neurotoxicity, coincidentally to the changes in COX-2 expression (Fig. 1*G*). Although whole-tissue PGE_2 deriving from COX-2 almost doubles after MPTP, ≈65% still originates from COX-1 (see Table 2). Unlike in ventral midbrain, levels of COX-2 mRNA, proteins, and catalytic activity in cerebellum (brain region unaffected by MPTP) and striatum were unaffected by MPTP administration (data not shown). Thus, COX-2, but not COX-1, is up-regulated in the MPTP mouse model.

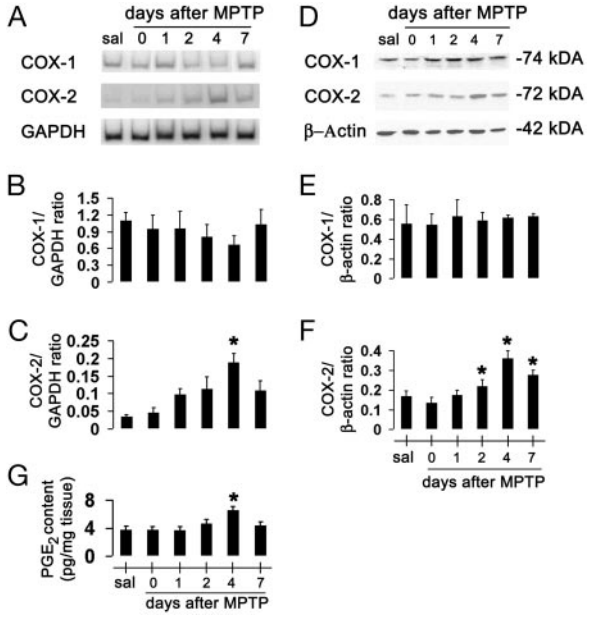

Fig. 1. Ventral midbrain COX-1 and COX-2 mRNA and protein expression after MPTP. COX-2 mRNA levels are increased by 4 days after MPTP injection (*A*) compared with controls (*C*), and almost return to basal levels by 7 days. COX-2 protein contents are minimal in saline-injected mice (sal) (*D*) but rise in a time-dependent manner after MPTP injection (*F*). COX-1 expression is not altered by MPTP (*A*, *B*, *D*, and *E*). Ventral midbrain PGE_2 levels are also increased 4 days after MPTP (*G*). Data are mean ± SEM for four to six mice per group. *, $P < 0.05$, compared with saline (Newman–Keuls post hoc test).

COX-2-Specific Induction in SNpc Dopaminergic Neurons After MPTP Administration. To elucidate the cellular origin of COX-2 up-regulation in the ventral midbrain of MPTP-treated mice, we performed immunohistochemistry. In saline controls, faint COX-2 immunoreactivity was seen in the neuropil (Fig. 2 *A* and *B*). In MPTP-treated mice, at 2 and 4 days after the last injection, ventral midbrain COX-2 immunostaining of the neuropil was increased and several COX-2-positive cells with a neuronal morphology were seen in the SNpc (Fig. 2 *C* and *D*). COX-2-positive neurons showed immunoreactivity over the cytoplasmic and nuclear areas (Fig. 2*D*), which is consistent with the known subcellular localization of this

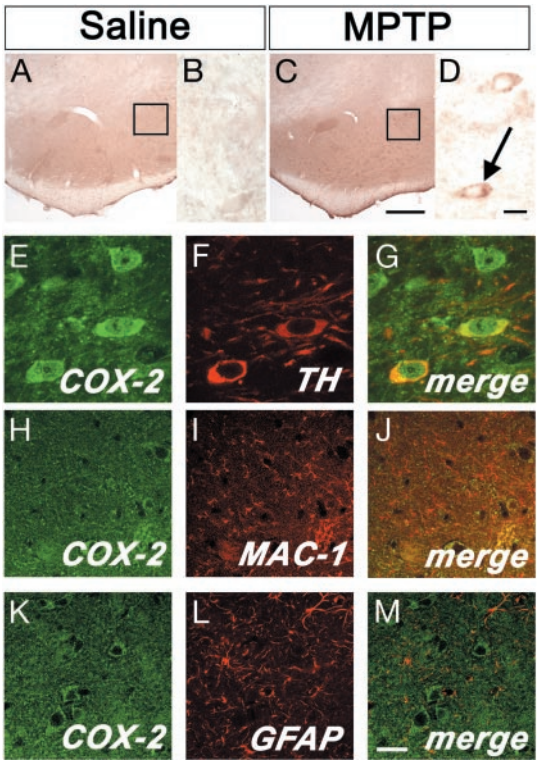

Fig. 2. Ventral midbrain illustration of COX-2 immunolocalization. No COX-2-positive cells are seen in saline-injected mice (*A* and enlarged *Inset* from *A* in *B*). Conversely, COX-2-positive cells are abundant after MPTP (*C* and enlarged *Inset* from *C* in *D*, arrow). Double immunofluorescence confirms that COX-2 (green) is highly expressed in TH-positive neurons (red; *E–G*) and not in MAC-1-positive cells (*H-J*; red) or GFAP-positive cells (*K–M*; red). [Scale bars, 250 μm (*A* and *C*), 10 μm (*B* and *D–G*), and 20 μm (*H–M*).]

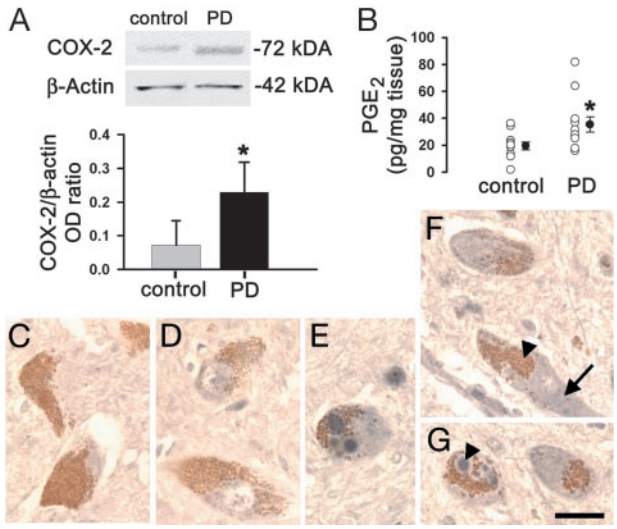

Fig. 3. Ventral midbrain COX-2 expression is minimal in normal human specimens but is increased 3-fold in PD samples (*A*). Ventral midbrain PGE_2 levels are also increased in PD (*B*). COX-2 (blue) is not detected in neuromelanized (brown) dopaminergic neurons in controls (*C* and *D*) but is well detected in PD (*E–G*). COX-2 immunostaining (*F*; *arrow*) is visible in cells with neuromelanin (*F*; arrowhead). COX-2 immunostaining is found in the core of a Lewy body (*G*; arrowhead). Data are mean ± SEM for 3–6 samples for COX-2 protein and 11 samples for PGE_2 assessment. *, $P < 0.05$, compared with normal controls (Newman–Keuls posthoc test). (Scale bar, 25 μm.)

enzyme (13). By double immunofluorescence, we found that ventral midbrain COX-2-positive cells were indeed neurons, among which almost all were dopaminergic (Fig. 2 *E–G*). COX-2 immunofluorescence did not colocalize with the microglial marker MAC-1 (Fig. 2 *H–J*), or with the astrocytic marker GFAP (Fig. 2 *K–M*). No difference in COX-2 immunoreactivity was observed in the striatum between saline- and MPTP-treated mice (data not shown). These data demonstrate that COX-2 is primarily up-regulated in ventral midbrain dopaminergic neurons during MPTP neurotoxicity.

COX-2 Up-Regulation in Postmortem Ventral Midbrain Samples from PD. To assess whether the changes in COX-2 seen after MPTP were present in PD, we assessed COX-2 protein and PGE_2 contents in postmortem SNpc samples. Consistent with the MPTP findings, PD samples had significantly higher contents of COX-2 protein and PGE_2 than normal controls (Fig. 3 *A* and *B*). As in the mice, no significant change in PGE_2 content was seen in the striatum of PD patients (data not shown). Histologically, cellular COX-2 immunoreactivity was not identified in a normal control (Fig. 3 *C* and *D*), but it was in PD midbrain sections, where it was essentially found in SNpc neuromelanized neurons (Fig. 3 *E–G*). Within these dopaminergic neurons, COX-2 immunostaining was seen in cytosol and in the typical intraneuronal proteinacious inclusions, Lewy bodies (Fig. 3*G*). The similarity of the COX-2 alterations between the MPTP mice and the PD postmortem specimens strengthens the value of using this experimental model to study the role of COX-2 in the PD neurodegenerative process.

Ablation of COX-2 Mitigates MPTP-Induced Neurodegeneration. In light of the MPTP- and PD-induced SNpc COX-2 up-regulation, we asked whether this enzyme is implicated in the nigrostriatal degeneration seen in these two pathological situations. Therefore, we compared the effects of MPTP in *Ptgs2*$^{-/-}$, *Ptgs2*$^{+/-}$, and *Ptgs2*$^{+/+}$ mice. Stereological counts of SNpc dopaminergic neurons defined by TH and Nissl staining did not differ among the three genotypes after saline injections (Fig. 4 *A* and *B* and Table 1). SNpc dopaminergic neuron numbers were reduced in all three genotypes after MPTP injections (Fig. 4 *A* and *B* and Table 1). However, in *Ptgs2*$^{-/-}$ mice, and to a lesser extent in *Ptgs2*$^{+/-}$ mice, significantly more TH- and Nissl-stained SNpc neurons survived MPTP administration than in *Ptgs2*$^{+/+}$ mice (Fig. 4*C* and Table 1). In the striatum, the density of TH-positive fibers was decreased to 16% of saline values in MPTP-treated *Ptgs2*$^{+/+}$ and to 21% in *Ptgs2*$^{+/-}$ mice, but only to 63% in *Ptgs2*$^{-/-}$ mice (Table 1). In contrast to the lack of COX-2, the lack of COX-1 did not decrease MPTP neurotoxicity: *Ptgs1*$^{-/-}$ mice [saline = 8,640 ± 725, MPTP = 4,247 ± 554 (mean ± SEM for three to eight mice per group)] and *Ptgs1*$^{+/+}$ littermates (saline = 8,577 ± 334, MPTP = 5,274 ± 147; $P > 0.05$, between MPTP-treated groups, Newman–Keuls posthoc test). Thus, COX-2, but not COX-1, participates in the MPTP neurotoxic process affecting dopaminergic cell bodies in the SNpc and nerve fibers in the striatum.

MPTP-Induced Toxicity Requires COX-2 Catalytic Activity. In the absence of catalytic activity, COX-2 can still exert deleterious effects in transfected cells (14). To test whether a similar situation occurs *in vivo* in the demise of dopaminergic neurons mediated by MPTP, nigrostriatal degeneration was assessed in regular mice injected with this neurotoxin and treated with the selective COX-2 inhibitor rofecoxib. The selected regimens of rofecoxib did not cause any distress in the animals (see *Materials and Methods* for details) or any alteration in MPTP metabolism (see below), and afforded meaningful brain accumulation (see *Materials and Methods* for details). At both 25 and 50 mg/kg, rofecoxib completely blocked ventral midbrain COX-2-derived PGE_2 production (see Table 2). In mice injected with MPTP that received either 25 or 50 mg/kg rofecoxib, ≈74% and 88%,

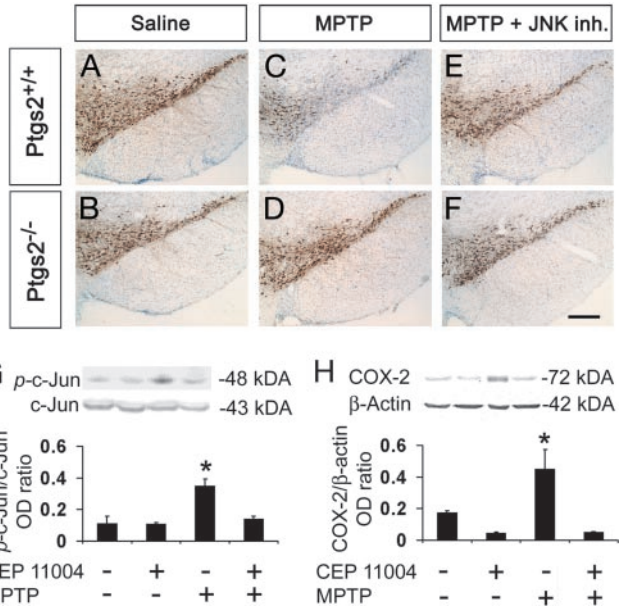

Fig. 4. Effect of COX-2 ablation and JNK pathway inhibition on MPTP-induced neuronal loss. TH-positive neuronal counts are shown in Table 1 and appear comparable between saline-injected *Ptgs2*$^{-/-}$ and *Ptgs2*$^{+/+}$ mice (*A* and *B* and Table 1). SNpc TH-positive neurons are more resistant to MPTP in *Ptgs2*$^{-/-}$ (*D*) than in *Ptgs2*$^{+/+}$ (*C*) mice, 7 days after MPTP injection. CEP-11004 protects *Ptgs2*$^{+/+}$ mice against MPTP neurotoxicity (*E*). Treatment of *Ptgs2*$^{-/-}$ mice with CEP-11004 does not enhance protection against MPTP (*F* and Table 1). (*G*) Ventral midbrain MPTP-induced c-Jun phosphorylation (*p*-c-Jun) inhibition by 1 mg/kg CEP-11004. (*H*) Ventral midbrain MPTP-induced COX-2 up-regulation is also inhibited by 1 mg/kg CEP-11004. Data are mean ± SEM for three to six mice per group. *, $P < 0.05$, compared with the other three groups (Newman–Keuls posthoc test). (Scale bar, 250 μm.)

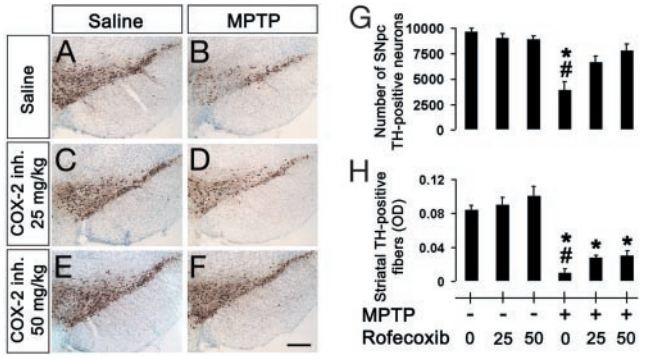

Fig. 5. TH-positive neurons and striatal fibers are more resistant to MPTP in mice treated with rofecoxib (25 or 50 mg/kg p.o.; *D* and *F*) than in mice receiving vehicle (*B*), 7 days after MPTP injection (SNpc neuronal counts are shown in *G* and striatal fiber optical density is shown in *H*). Rofecoxib by itself has no effect on TH-positive neurons (*A*, *C*, and *E*). Data are mean ± SEM for three to six mice per group. *, $P < 0.05$, compared with saline-treated controls; #, $P < 0.05$, compared with rofecoxib-treated MPTP animals (Newman–Keuls posthoc test). (Scale bar, 250 μm.)

respectively, of SNpc TH-positive neurons survived, compared with 41% in mice injected with MPTP only (Fig. 5 *C*–*G*). Similarly, both doses of rofecoxib attenuated the loss of TH-positive fibers caused by MPTP (Fig. 5*H*) in a dose-dependent manner, although this beneficial effect was less profound than was seen with COX-2 ablation (Table 1). These findings demonstrate how crucial the enzymatic function of COX-2 is to its neurotoxic effects on at least SNpc dopaminergic neurons.

JNK Activation Controls COX-2 Induction During MPTP-Induced Death. Stress-activated protein kinase JNK can regulate COX-2 transcription in mammalian cells (15). We therefore investigated whether MPTP-induced COX-2 up-regulation is a JNK-dependent event. After MPTP administration to mice there was a robust ventral midbrain activation of JNK, as evidenced by c-Jun phosphorylation (Fig. 4*G*) and, as shown above, a marked up-regulation of COX-2 (Fig. 4*H*). Conversely, in mice in which JNK activation was blocked by 1 mg/kg CEP-11004, MPTP caused almost no c-Jun phosphorylation and no COX-2 up-regulation (Fig. 4 *G* and *H*), thus demonstrating the critical role of the JNK/c-Jun pathway in MPTP-mediated COX-2 induction.

Administration of CEP-11004 at 1 mg/kg decreased MPTP-induced SNpc dopaminergic neuronal death, but failed to attenuate striatal dopaminergic fiber loss in *Ptgs2*$^{+/+}$ mice (Fig. 4 *C* and *E* and Table 1). The magnitude of neuroprotection against MPTP provided by the lack of COX-2 did not differ between CEP-11004-treated and untreated *Ptgs2*$^{-/-}$ mice (Fig. 4 *D* and *F* and Table 1). These data show that although both blockade of JNK and lack of COX-2 attenuate MPTP-induced SNpc dopaminergic neuronal death, the combination of the two strategies does not enhance neuroprotection.

COX-2 Ablation and Inhibition Do Not Impair MPTP Metabolism. The main determining factors of MPTP neurotoxic potency are its conversion in the brain to MPP^+ followed by MPP^+ entry into dopaminergic neurons and its subsequent blockade of mitochondrial respiration (16). To ascertain that resistance to the neurotoxic effects of MPTP provided by COX-2 ablation or inhibition was not because of alterations in any of these three key MPTP neurotoxic steps, we measured striatal levels of MPP^+ 90 min after the last injection of MPTP, striatal uptake of [^{3}H]MPP^+ into synaptosomes, and striatal MPP^+-induced lactate production, a reliable marker of mitochondrial inhibition (17). Striatal levels of MPP^+ were not lower in MPTP-injected *Ptgs2*$^{-/-}$ mice compared with *Ptgs2*$^{+/+}$ mice, regardless of whether or not mice received the JNK pathway inhibitor (see Table 3). Striatal levels of MPP^+ did not differ between MPTP-injected regular mice that either received or did not receive rofecoxib (see Table 3). The absence of the COX-2 gene or the presence of rofecoxib up to 32 μM did not affect MPP^+-induced lactate production (lactate in μM/100 mg of protein: *Ptgs2*$^{+/+}$ = 56.1 ± 1.9, *Ptgs2*$^{-/-}$ = 58.6 ± 5.2; regular mice/vehicle = 60.8 ± 3.8, regular mice/rofecoxib = 53.8 ± 7.3;

Table 1. Effect of COX-2 ablation and JNK pathway inhibition on MPTP toxicity

	SNpc: no. of TH-positive neurons			Striatum: TH-positive fibers, OD × 100		
Treatment	*Ptgs2*$^{+/+}$	*Ptgs2*$^{+/-}$	*Ptgs2*$^{-/-}$	*Ptgs2*$^{+/+}$	*Ptgs2*$^{+/-}$	*Ptgs2*$^{-/-}$
Saline	9,153 ± 328	9,104 ± 643	9,200 ± 643	11.9 ± 2.7	12.2 ± 1.9	11.5 ± 1.9
MPTP	5,228 ± 283*†‡	6,296 ± 356*‡	7,600 ± 610	1.9 ± 1.0*‡	2.6 ± 0.6*‡	7.3 ± 0.4
MPTP/CEP-11004	6,933 ± 501	—	8,420 ± 799	2.4 ± 0.5*‡	—	7.4 ± 0.3

Values are mean ± SEM for four to eight mice per group. *, $P < 0.05$ compared with the other groups of saline-treated mice; †, $P < 0.05$ compared with MPTP-injected *Ptgs2*$^{+/+}$ mice treated with the JNK pathway inhibitor CEP-11004; ‡, $P < 0.05$ compared with all three groups of *Ptgs2*$^{-/-}$ mice.

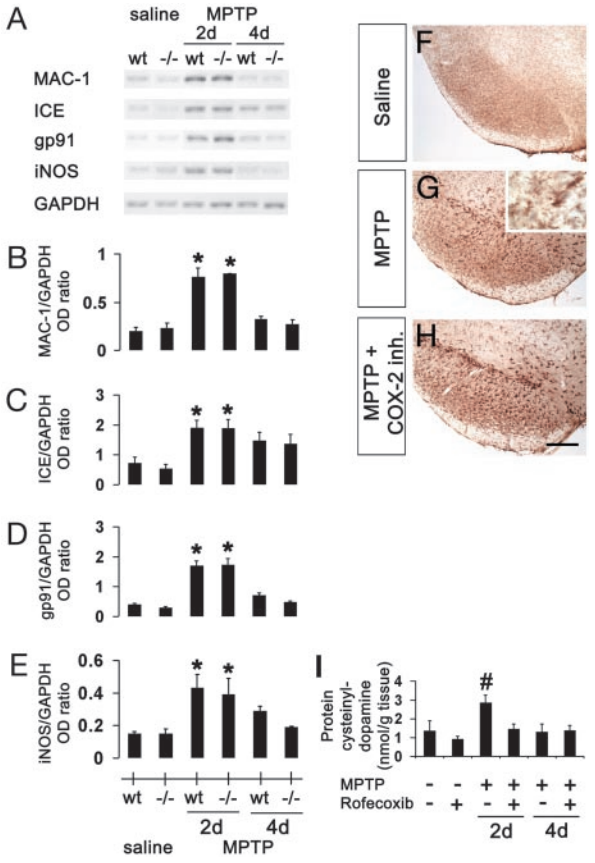

Fig. 6. Expression of inflammatory and oxidative stress markers after MPTP. Two days after MPTP injection, mRNA expression of MAC-1 (*A* and *B*), ICE (*A* and *C*), gp91 (*A* and *D*), and iNOS (*A* and *E*) are increased in the ventral midbrain and none is attenuated by COX-2 ablation. MAC-1 immunoreactivity is minimal in saline-injected mice in ventral midbrain (*F*), but is increased after MPTP injection (*G*; *Inset* shows MPTP-induced microglial activation at higher magnification). (*H*) COX-2 inhibition does not attenuate MPTP-induced microglial activation. (*I*) MPTP increases ventral midbrain protein-bound cysteinyl-dopamine, which is blocked by rofecoxib. Data are mean ± SEM for four to six mice per group. *, $P <$ 0.05, compared with saline treated groups; #, $P < 0.05$, compared with the other five groups (Newman–Keuls posthoc test). (Scale bar, 250 μm.)

mean ± SEM for six mice per group). Striatal uptake of [^{3}H]MPP$^+$ was not impaired in *Ptgs2*$^{-/-}$ mice, compared with *Ptgs2*$^{+/+}$ mice, with an IC_{50} of 226.3 ± 21 nM for *Ptgs2*$^{-/-}$ mice and 195.3 ± 6.38 nM for their wild-type littermates (mean ± SEM for three mice per group). These findings suggest that COX-2-mediated neurotoxicity during MPTP-induced neuronal death operates either in parallel or downstream to MPTP's key metabolic steps.

COX-2 Modulation Does Not Alleviate MPTP-Associated Microglial Activation. Given the proinflammatory role of prostanoids such as PGE_2, we investigated the potential involvement of SNpc dopaminergic neuron production of prostaglandins in MPTP-associated microglial activation. As shown before (11, 18), there is a robust microglial activation in mice after MPTP administration. This activation was evidenced by increased contents of MAC-1, iNOS, gp91, and ICE mRNAs in ventral midbrains (Fig. 6 *A–E*), as well as by increased numbers of MAC-1-positive cells in both SNpc (Fig. 6*G*) and striatum (data not shown). Whereas both COX-2 abrogation and inhibition attenuated MPTP-mediated death, neither prevented the microglial response described above (RT-PCR: Fig. 6 *A–E*, data not shown for COX-2 inhibition; immunostaining for MAC-1: Fig. 6 *F–H*; data not shown for COX-2 ablation). Thus, COX-2 plays a negligible role in the microglial activation and the production of microglial-derived noxious factors after MPTP intoxication.

COX-2 Mediates Oxidative Stress During MPTP-Induced Neurodegeneration. Aside from production of extracellular prostanoids, COX-2 can also damage intracellular protein-bound sulfhydryl groups through the oxidation of catechols such as dopamine (19). To investigate whether such a mechanism is in play here, we quantified ventral midbrain content of protein 5-cysteinyl-dopamine, a stable modification engendered by the COX-related oxidation of dopamine (19). In saline-injected mice, baseline levels of protein 5-cysteinyl-dopamine were slightly lower in mice treated than those not treated with rofecoxib (Fig. 6*I*). In MPTP-injected mice that did not receive rofecoxib, protein 5-cysteinyl-dopamine levels were >2-fold higher than in their saline-injected counterparts (Fig. 6*I*). In contrast, in MPTP-injected mice that did receive rofecoxib, there was no significant increase in protein 5-cysteinyl-dopamine levels compared with their saline controls (Fig. 6*I*).

Discussion

This study shows an up-regulation of COX-2 in the brain regions that house nigrostriatal dopaminergic neurons in both MPTP mice and human PD samples. Increased COX-2 expression was associated with increased PGE_2 tissue content, thus indicating that the increased COX-2 is catalytically active. However, we found that ventral midbrain PGE_2 reflects mainly COX-1 activity in both normal and MPTP-injured mice. Although affected brain regions in MPTP and PD are cellularly heterogeneous, conspicuous COX-2 immunoreactivity was essentially found in SNpc dopaminergic neurons from MPTP-treated mice and postmortem PD samples. This finding raises the possibility that COX-2 up-regulation could amplify the neurodegenerative process specifically in SNpc dopaminergic neurons, thus rendering these neurons more prone than any other neurons to succumb to MPTP toxicity or PD injury.

Consistent with the involvement of COX-2 in MPTP and PD neurodegenerative processes, approximately twice as many SNpc dopaminergic neurons and striatal dopamine fibers survived in *Ptgs2*$^{-/-}$ mice compared with their wild-type littermates after MPTP administration. These results agree with the previous demonstrations that COX-2 modulation mitigates MPTP-mediated SNpc dopaminergic neurotoxicity in mice (20, 21). Because COX-2 can also exert deleterious effects unrelated to its catalytic activity (14), it must be noted that lack of COX-2 protein and inhibition of COX-2 by rofecoxib produced comparable protection of SNpc dopaminergic neurons against MPTP; striatal dopaminergic fibers were better protected by COX-2 ablation than by inhibition. It can thus be concluded that the deleterious effect of COX-2, at least on SNpc dopamine neurons in the MPTP model, and probably in PD, relies on COX-2 catalytic activity. Unlike ablation of COX-2, ablation of COX-1 failed to produce any protection against MPTP, thus indicating that induction of COX-2 expression, but not COX-1 or COX-1 gene products (e.g., COX-3; ref. 22), is instrumental in MPTP neurotoxicity.

Our data confirm the activation of the JNK/c-Jun signaling pathway after MPTP administration (23) and demonstrate that the blockade of this pathway by CEP-11004 at a concentration that inhibits c-Jun phosphorylation also inhibits COX-2 induction. In mice lacking both JNK-2 and JNK-3 genes, we found that MPTP fails to cause any phosphorylation of c-Jun or induction of COX-2 (S.H., M.V., P.T., R.J. Davis, S.P., E.C. Hirsch, P. Rakic, and R. A. Flavell, unpublished data). These results support a critical role for the JNK/c-Jun signaling pathway in the regulation of COX-2 expression in SNpc dopaminergic neurons after MPTP administration. However, COX-2 ablation attenuated MPTP-induced SNpc dopaminergic neuronal and striatal dopaminergic fiber loss, whereas JNK pathway inhibition protected only against SNpc neuronal death. This finding suggests that, in the absence of any COX-2 induction, residual COX-2 proteins in CEP-11004-treated

mice suffice to damage at least striatal dopaminergic fibers, which are more sensitive to MPTP than to SNpc dopaminergic neurons. We also show that the combination of JNK blockade and COX-2 ablation did not confer neuroprotection against MPTP beyond that produced by COX-2 ablation alone. It can thus be concluded that among the host of genes regulated by JNK, COX-2 may be the mediator of JNK's deleterious effects on SNpc dopaminergic neurons in the MPTP model of PD.

COX-2 toxicity is presumably mediated by its production of inflammatory prostanoids. Accordingly, neurons expressing COX-2 would cause their own demise through a harmful interplay with glial cells: COX-2-positive neurons release PGE_2, which promotes the production of microglial-derived mediators, which, in turn, help in killing neurons. Although we have previously demonstrated that activated microglia and derived factors do amplify MPTP-induced neurodegeneration (11), the present study shows that COX-2 modulation alters neither the morphological nor the functional correlates of microglial activation after MPTP administration. Therefore, neuronal COX-2 cytotoxicity in this model of PD does not appear to be linked to the inflammatory response. This view is consistent with our finding that most of the ventral midbrain PGE_2 originates not from COX-2, but from COX-1.

Alternatively, neuronal COX-2 overexpression may kill neurons in a cell-autonomous manner (5, 6, 24). Relevant to the leading pathogenic hypothesis for PD (25) is the fact that COX-2 cell-autonomous toxicity may arise from the formation of reactive oxygen species generated during COX peroxidase catalysis of PGG_2 conversion to PGH_2 (26). On donation of electrons to COX, cosubstrates such as dopamine become oxidized to dopamine-quinone (19), which is highly reactive with glutathione and protein amino acids such as cysteine, tyrosine, and lysine. Supporting the occurrence of such an oxidative process after MPTP injection is the marked increase in ventral midbrain protein cysteinyl-dopamine content, a fingerprint of protein cysteinyl attack by dopamine-quinone (19), in MPTP-intoxicated mice. We also demonstrated the COX-2 dependency of this toxic event by showing that COX-2 inhibition prevented the rise in protein cysteinyldopamine seen after MPTP injections. The deleterious consequences of dopamine-quinone can include depletion of vital antioxidants such as glutathione, inactivation of critical enzymes such as TH (27), and accumulation of α-synuclein protofibrils, a proposed key event in PD pathogenesis (28). Given these findings, it is thus undeniable that COX-2 up-regulation in SNpc dopaminergic neurons can unleash an array of oxidative assaults, which ultimately may play a decisive role in determining the fate of these neurons in the MPTP model and in PD itself.

Collectively, our data provide evidence for COX-2 up-regulation in MPTP and PD and support a significant role for COX-2 in both the mechanism and the specificity of MPTP- and PD-induced SNpc dopaminergic neuronal death. The present study suggests that inhibition of COX-2 may be a valuable target for the development of new therapies for PD aimed at slowing the progression of the neurodegenerative process.

We thank Dr. Robert E. Burke and Dr. M. Kerry O'Banion for their advice and insightful comments on the manuscript; Mrs. Birgit C. Teismann and Mr. Brian Jones for their help in the preparation of this manuscript; Dr. W. L. Smith (Michigan State University) for providing us with the COX-2 antibody; Merck for providing rofecoxib; Cephalon for supplying CEP-11004; Mrs. Pauline Luk (Merck) for the rofecoxib measurements; and the Columbia University Brain Bank for providing the human postmortem samples. This work was supported by National Institutes of Health/National Institute of Neurological Disorders and Stroke Grants NS37345, NS38586, NS42269, NS11766-27A1, and NS38370, U.S. Department of Defense Grants DAMD 17-99-1-9471 and DAMD 17-03-1, the Lowenstein Foundation, the Lillian Goldman Charitable Trust, and the Parkinson's Disease Foundation. P.T. is a recipient of Scholarship DFG TE 343/1-1 from the German Research Foundation.

1. Fahn, S. & Przedborski, S. (2000) in *Merritt's Neurology*, ed. Rowland, L. P. (Lippincott, Williams & Wilkins, New York), pp. 679–693.
2. Przedborski, S., Kostic, V., Giladi, N. & Eidelberg, D. (2003) in *Dopamine Receptors and Transporters*, eds. Sidhu, A., Laruelle, M. & Vernier, P. (Dekker, New York), pp. 363–402.
3. Wyss-Coray, T. & Mucke, L. (2000) *Nat. Med.* **6,** 973–974.
4. Almer, G., Guegan, C., Teismann, P., Naini, A., Rosoklija, G., Hays, A. P., Chen, C. & Przedborski, S. (2001) *Ann. Neurol.* **49,** 176–185.
5. Andreasson, K. I., Savonenko, A., Vidensky, S., Goellner, J. J., Zhang, Y., Shaffer, A., Kaufmann, W. E., Worley, P. F., Isakson, P. & Markowska, A. L. (2001) *J. Neurosci.* **21,** 8198–8209.
6. Nogawa, S., Zhang, F., Ross, M. E. & Iadecola, C. (1997) *J. Neurosci.* **17,** 2746–2755.
7. O'Banion, M. K. (1999) *Crit. Rev. Neurobiol.* **13,** 45–82.
8. Morham, S. G., Langenbach, R., Loftin, C. D., Tiano, H. F., Vouloumanos, N., Jennette, J. C., Mahler, J. F., Kluckman, K. D., Ledford, A. & Lee, C. A. (1995) *Cell* **83,** 473–482.
9. Przedborski, S., Jackson-Lewis, V., Naini, A., Jakowec, M., Petzinger, G., Miller, R. & Akram, M. (2001) *J. Neurochem.* **76,** 1265–1274.
10. Murakata, C., Kaneko, M., Gessner, G., Angeles, T. S., Ator, M. A., O'Kane, T. M., McKenna, B. A., Thomas, B. A., Mathiasen, J. R., Saporito, M. S., *et al.* (2002) *Bioorg. Med. Chem. Lett.* **12,** 147–150.
11. Wu, D. C., Jackson-Lewis, V., Vila, M., Tieu, K., Teismann, P., Vadseth, C., Choi, D. K., Ischiropoulos, H. & Przedborski, S. (2002) *J. Neurosci.* **22,** 1763–1771.
12. LaVoie, M. J. & Hastings, T. G. (1999) *J. Neurochem.* **73,** 2546–2554.
13. Spencer, A. G., Woods, J. W., Arakawa, T., Singer, I. I. & Smith, W. L. (1998) *J. Biol. Chem.* **273,** 9886–9893.
14. Trifan, O. C., Smith, R. M., Thompson, B. D. & Hla, T. (1999) *J. Biol. Chem.* **274,** 34141–34147.
15. Subbaramaiah, K., Chung, W. J. & Dannenberg, A. J. (1998) *J. Biol. Chem.* **273,** 32943–32949.
16. Przedborski, S., Jackson-Lewis, V., Djaldetti, R., Liberatore, G., Vila, M., Vukosavic, S. & Almer, G. (2000) *Restor. Neurol. Neurosci.* **16,** 135–142.
17. Kindt, M. V., Heikkila, R. E. & Nicklas, W. J. (1987) *J. Pharmacol. Exp. Ther.* **242,** 858–863.
18. Liberatore, G., Jackson-Lewis, V., Vukosavic, S., Mandir, A. S., Vila, M., McAuliffe, W. J., Dawson, V. L., Dawson, T. M. & Przedborski, S. (1999) *Nat. Med.* **5,** 1403–1409.
19. Hastings, T. G. (1995) *J. Neurochem.* **64,** 919–924.
20. Teismann, P. & Ferger, B. (2001) *Synapse* **39,** 167–174.
21. Feng, Z., Wang, T., Li, D., Fung, P., Wilson, B., Liu, B., Ali, S., Langenbach, R. & Hong, J. (2002) *Neurosci Lett.* **329,** 354–358.
22. Chandrasekharan, N. V., Dai, H., Roos, K. L., Evanson, N. K., Tomsik, J., Elton, T. S. & Simmons, D. L. (2002) *Proc. Natl. Acad. Sci. USA* **99,** 13926–13931.
23. Saporito, M. S., Thomas, B. A. & Scott, R. W. (2000) *J. Neurochem.* **75,** 1200–1208.
24. Mirjany, M., Ho, L. & Pasinetti, G. M. (2002) *J. Pharmacol. Exp. Ther.* **301,** 494–500.
25. Przedborski, S. & Jackson-Lewis, V. (2000) in *Free Radicals in Brain Pathophysiology*, eds. Poli, G., Cadenas, E. & Packer, L. (Dekker, New York), pp. 273–290.
26. Smith, W. L., Marnett, L. J. & DeWitt, D. L. (1991) *Pharmacol. Ther.* **49,** 153–179.
27. Kuhn, D. M., Arthur, R. E., Jr., Thomas, D. M. & Elferink, L. A. (1999) *J. Neurochem.* **73,** 1309–1317.
28. Conway, K. A., Rochet, J. C., Bieganski, R. M. & Lansbury, P. T., Jr. (2001) *Science* **294,** 1346–1349.